Journal of Electroanalytical Chemistry 707 (2013) 20–30

Contents lists available at ScienceDirect

Journal of Electroanalytical Chemistry

journal homepage: www.elsevier.com/locate/jelechem

Cyclic multipulse voltammetric techniques. Part I: Kinetics of electrode processes

Dijana Jadreško *, Marina Zelić

Division for Marine and Environmental Research, Ruđer Bošković Institute, P.O. Box 180, HR-10002 Zagreb, Croatia

ARTICLE INFO

Article history:
Received 3 April 2013
Received in revised form 5 August 2013
Accepted 6 August 2013
Available online 29 August 2013

Keywords:
Cyclic multi pulse voltammetry
Cyclic differential multi pulse voltammetry
Cyclic square-wave voltammetry
Excitation signal
Kinetics
Theory

ABSTRACT

A comparative, theoretical and experimental, analysis of reversible and kinetically controlled electrode reactions by cyclic multi pulse voltammetry (CMPV), cyclic differential multi pulse voltammetry (CDMPV) and cyclic square-wave voltammetry (CSWV) is presented. The cyclic multipulse voltammetric techniques enable faster and more complete characterization of the electrode processes, comparing with classical multipulse voltammetric techniques. Electron transfer coefficients (α and β), i.e. symmetry of the electron transfer reaction can be estimated by visual inspection of the proper cyclic multipulse voltammogram. Their values, as well as the standard rate constant of a simple electrode reaction $Ox + ne^- \rightleftarrows Red$, can be determined from the slopes of linear dependences of characteristic (half wave or peak) cathodic and anodic potentials on the logarithm of pulse duration in CMPV and CDMPV, or logarithm of frequency in CSWV. The criteria for recognition of kinetically controlled electrode reactions by cyclic multipulse voltammetric techniques are given.

1. Introduction

The theoretical basis of pulse voltammetric techniques was defined more than 50 years ago [1]. Instead of a simple potential ramp (used in classical dc measurements) a sequence of potential pulses and current sampling at the end of each step were introduced. In such a way, reduction of the charging current and consequently lowering of detection limits were achieved. Experimental application of pulse techniques started soon after defining of their foundation. Major progress, however, was related to development of computers, microprocessors and advanced software packages [2].

In the late seventies Ryan [3] developed a theory of cyclic staircase voltammetry (CSV) for the study of kinetics and mechanisms of electrode processes. During the last three decades, cyclic staircase voltammetry became a very popular and universal technique for initial electrochemical characterization of unknown systems. It is characterized by stepwise change of the electrode potential in negative and then to positive direction (in the case of reduction processes), without application of pulses [4]. On the other hand, modern pulse voltammetric techniques include stepwise excitation signals to which potential pulses are superimposed with scanning in only one direction. However, an electrode process initially studied in such a way could be additionally analyzed by applying the inverse scan direction [5–10]. Finally, the two independent techniques ("classical" and "inverse") could be combined by applying cyclic multi pulse voltammetry.

The cyclic potential-time waveform in differential pulse voltammetry (DPV) and its advantages compared to CSV (i.e. better resolution of DPV peaks and easier measurements of their heights and potentials) were first described by Drake et al. [11]. However, the authors applied negative pulses in both scan directions. The theory of cyclic square-wave voltammetry (CSWV) and its experimental verification were first reported by Xinsheng and Guogang [12]. They studied reversible and quasireversible processes whereas Camacho et al. [13] were focused on amalgam forming electrode reactions. Molina et al. [14] presented the study of reversible redox reaction of a molecule containing n electroactive redox centers using the same technique. Furthermore, Helfrick and Bottomley [15] developed a theory for single and consecutive reversible electron transfer reactions and examined the electroanalytical/kinetic applications of CSWV. As far as we know, articles about cyclic pulse voltammetry (CPV) do not exist. The main reason for rather small number of papers concerning the mentioned techniques is an experimental problem. Until recently, the most often used instruments/potentiostats and software packages, did not offer such measurements. However, things have changed. Recently developed instruments with electrochemical software "NOVA" offer the possibility of creating/programming desired voltammetric technique, i.e. implementation of the particular cyclic pulse voltammetric technique in experimental work.

According to a recent recommendation [16] the studied techniques should be named in a somewhat different manner, i.e. as

* Corresponding author. Tel.: +385 14561181.
E-mail address: djadresko@irb.hr (D. Jadreško).

1572-6657/$ - see front matter © 2013 Elsevier B.V. All rights reserved.
http://dx.doi.org/10.1016/j.jelechem.2013.08.011

different types of cyclic multipulse voltammetry. In the present communication, the signals that arise from the application of cyclic multipulse voltammetry (CMPV), cyclic differential multipulse voltammetry (CDMPV) and cyclic square-wave voltammetry (CSWV) are simulated. These techniques are based on the potential-time waveforms defined in Fig. 1. They were introduced to experimental work by using electrochemical software "NOVA" (version 1.5 or higher, from Metrohm Autolab). Theoretical and experimental possibilities for study and recognitions of various kinetic and diffusion controlled electrode processes, as well as the influence of timing/kinetic parameters on the voltammograms (i.e. characteristic potential, height and shape of the signal) were investigated. It is expected that the cyclic multipulse techniques enables faster, easier and more complete characterization of the electrode process (that is determination of the k_s, α, β, D, $E^{0'}$, etc.), compared to classic multipulse voltammetric techniques.

The experimental results are compared with theoretically obtained relationships. From such analyses, there arise simple diagnostic criteria for elucidation of the kinetics of electrode reactions.

2. Experimental

All electrolyte solutions were prepared from the reagent grade chemicals and water purified in a Milipore Mili-Q system. For preparation of the uranyl(VI) stock solution, the classical procedure given in Gmelin's handbook [17] was applied. The starting salt for all solutions of Eu^{3+} was $Eu(NO_3)_3 \times 5H_2O$ (Fluka).

All voltammograms were recorded using a static mercury drop electrode (663 VA Stand from Metrohm). A glassy carbon rod served as a counter electrode whereas all potentials were given with respect to Ag/AgCl (3 mol/L KCl) with 3 mol/L NaCl in the electrolyte bridge (to prevent formation of sparingly soluble $KClO_4$

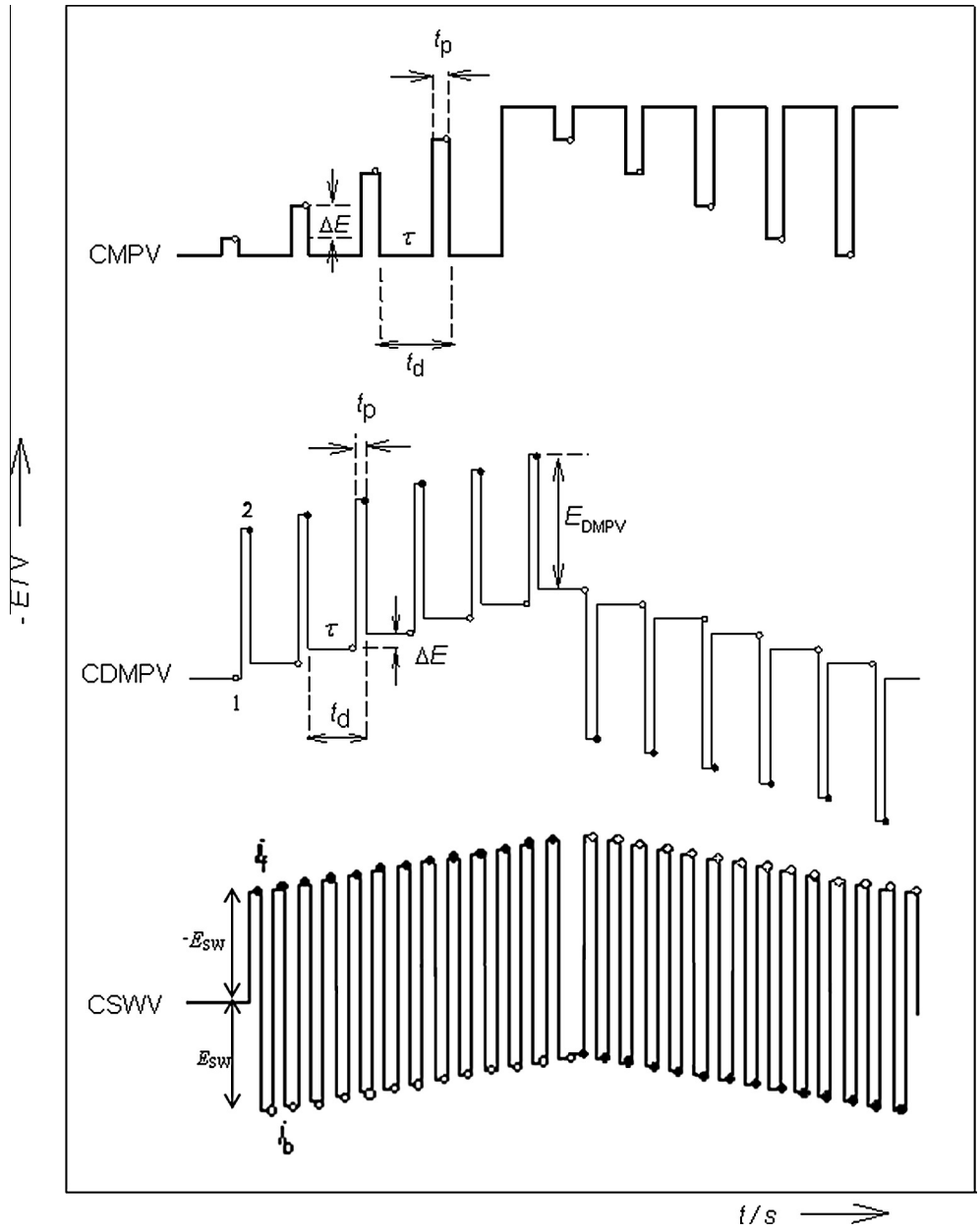

Fig. 1. Excitation signals in cyclic multi pulse (CMPV), cyclic differential multi pulse (CDMPV) and cyclic square-wave voltammetry (CSWV). Sampling points are schematically indicated for each technique. ΔE = step potential, t_d = interval time, t_p = pulse time, $E_{DMPV/SWV}$ = pulse amplitude, τ = time between pulses ($\tau = t_d - t_p$).

in the frit). The electrode system was attached trough the corresponding IME module to the "PGSTAT 101" instrument (from Eco Chemie, Utrecht), controlled by the electrochemical software "NOVA".

The advantage of this software package is that it provides complete control over the experiment (i.e. flexibility in setting). More exactly, "NOVA" offers the possibility of performance of more electrochemical techniques one after another (with or without "pause" between them), according to the requirements of the user [18]. Thus, the above mentioned techniques were programed and experimentally used.

Before starting each new set of measurements, the solution in the electrolytic cell was deaerated with high purity (99.999%) nitrogen for 15 min. The room temperature was maintained at 25 ± 1 °C.

3. A model

A simple, reversible or kinetically controlled electron transfer reaction on the stationary, planar electrode is considered:

$$\mathrm{Ox} + ne^- \rightleftarrows \mathrm{Red} \quad (1)$$

It is assumed that both the reactant Ox and the product Red are soluble in the aqueous electrolyte phase and are not adsorbed on the electrode surface. Initially only the reactant is present in the solution. The mass transport is solved by digital simulation, using a common dimensionless diffusion coefficient $D\Delta t/\Delta x^2 = 0.4$, where Δt and Δx are time and space increments, respectively [19]. The meanings of all symbols are listed in Table 1. The time increment is defined as: $\Delta t = t_p/25$ (in CDMPV and CSWV) or $\Delta t = t_p/50$ (in CMPV).

In the case of a kinetically controlled electrode reaction (1), current response generally depends on the cathodic transfer coefficient α and the dimensionless kinetic parameter κ ($\kappa = k_s(t_p/D)^{1/2}$ in CMPV and CDMPV, or $\kappa = k_s(Df)^{-1/2}$ in CSWV). The conditions at the electrode surface are defined by Nernst (in the case of reversible electrode reaction) or Butler–Volmer equation (in the case of a kinetically controlled electron transfer reaction). A program written in Quick Basic is available on request.

In cyclic multipulse techniques the current is measured at the end of each pulse (Fig. 1), and plotted as a function of the corresponding potential (pulse in CMPV, or the staircase in CDMPV and CSWV). In theory, the dimensionless current is calculated: $\Phi = i(\pi t_p)^{1/2}(nFSc^*_{Ox}D^{1/2})^{-1}$ (in CPV and CDPV) and $\Phi = i(nFSc^*_{Ox})^{-1}(Df)^{-1/2}$ (in CSWV).

Table 1
List of symbols.

α	Cathodic transfer coefficient
β	Anodic transfer coefficient
c^*_{Ox}	Bulk concentration of the reactant
D	Common diffusion coefficient
ΔE	Step potential
E	Electrode potential
$E^{0'}$	Formal potential
E^0	Standard potential
$E_{1/2,(r)c}$	Cathodic half-wave potential (for reverse/positive scan direction)
$E_{1/2,(r)a}$	Anodic half-wave potential (for reverse/positive scan direction)
$\Delta E_{1/2}$	Difference between anodic and cathodic half-wave potentials in CMPV
E_S	Switching potential
E_{st}	Starting potential
E_1	"prepulse" (staircase) electrode potential in CDMPV
E_2	"pulse" electrode potential in CDMPV
$E_{1,2} = (E_1 + E_2)/2$	"medium" electrode potential in CDMPV
$E_{SW/DPV}$	Square-wave/differential multipulse amplitude
E_p	Peak potential
ΔE_p	Difference between the anodic and cathodic peak potentials
f	Square-wave frequency
F	Faraday constant
Φ	Dimensionless current
Φ_1	Dimensionless "prepulse" component of net current in CDMPV
Φ_2	Dimensionless "pulse" component of net current in CDMPV
Φ_f	Dimensionless forward component of net current in CSWV
Φ_b	Dimensionless backward component of net current in CSWV
$\Delta\Phi_p$	Dimensionless net peak current
i	Current
$i_{d,c/a}$	Diffusion cathodic/anodic current
Δi	Net current
k_s	Standard rate constant
κ	Dimensionless kinetic parameter
κ_0	Critical kinetic parameter
n	Number of electrons
R	Gas constant
S	Electrode surface area
T	Absolute temperature
t	Time
t_p	Pulse time
$t_{p,0}$	Critical pulse duration
t_d	Interval time
τ	Time between pulses
Δt	Time increment
Δx	Space increment

4. Results and discussion

4.1. A reversible electrode reaction

The term "cyclic", in cyclic multi pulse voltammetry (CMPV), cyclic differential multi pulse voltammetry (CDMPV) and cyclic square-wave voltammetry (CSWV), means that the mentioned techniques are "formal" combinations of two independent measurements: "classical" and "reverse". In other words, more information about the electrode process can be obtained from one cyclic multipulse voltammogram than from two independent measurements ("classical" and "reverse"). Therefore it could be said that the cyclic multi pulse voltammetry is a time-saving technique.

The mentioned "definition" of cyclic techniques is really valid for CDMPV and CSV. With CMPV, however, the situation is more complicated. When forward scan is applied the initial potential (i.e. potential between pulses) is chosen so that no reduction of the reactant Ox occurs. On the other hand, for reverse scan the initial potential is set at a value from the limiting (reduction) dc current (i.e. 400 mV more negative than $E^{0'}$). Thus, during the long period τ ($t_d - t_p$, where $t_p \ll t_d$) when the potential is at E_{st} (or E_S), concentration of the electroactive reactant, Ox (or Red), on the electrode surface is almost maximal. Such design of experiments is in accordance with theory of NPV [20–22] and RPV [5–7,20]. Strictly speaking, however, CMPV cannot be treated as a simple "combination" of the two techniques. It is because, only in RPV, renewal of the initial conditions is achieved by waiting at a well defined potential. Because of this additional step, there is a difference between potential time waveforms of RPV [23] and the reverse branch of CMPV (Fig. 1). Its influence on theoretical or experimental signals depends on the applied measuring conditions and properties of the studied electrode process.

The cyclic multipulse voltammogram of a simple reversible electrode reaction (1) consists of two waves: forward/reduction and backward/(re)oxidation (Fig. 2A). Additionally, a sharp decrease of the reduction current at the switching potential ($E_S = -E_{st}$) could be observed.

In cyclic differential multi pulse voltammetry (CDMPV) excitation signal includes continuous stepwise change of the electrode

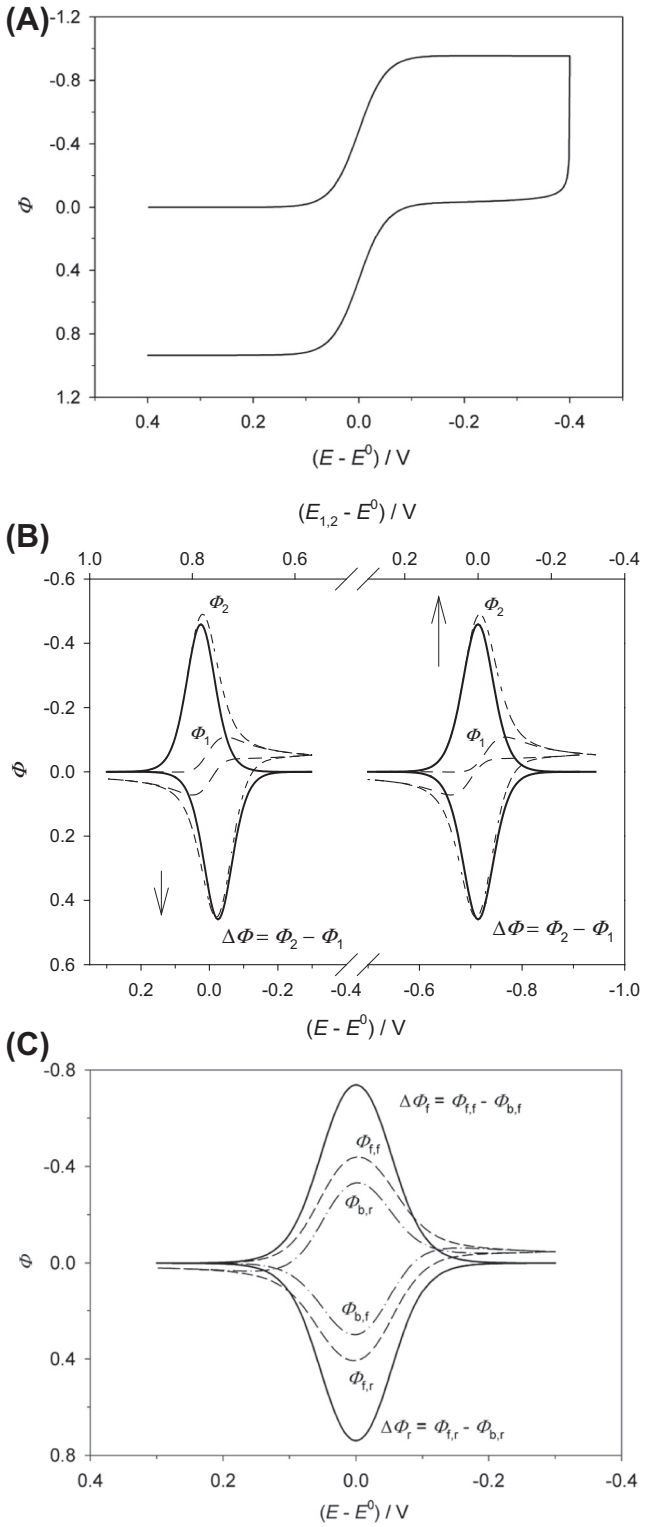

Fig. 2. Theoretical (A) cyclic multipulse voltammogram, (B) cyclic differential multipulse voltammogram (along with "prepulse" (Φ_1) and "pulse" (Φ_2) components of net current) and (C) cyclic square-wave voltammogram (along with forward (Φ_f) and backward (Φ_b) components of net current) of electrode reaction (1); n = 1. (A) t_d = 0.4 s, t_p = 50 ms, ΔE = 2 mV; (B) t_d = 0.15 s, t_p = 25 ms, E_{DMPV} = 50 - mV, ΔE = 5 mV, $\Phi = \frac{i\sqrt{\pi t_p}}{nFS\sqrt{Dc_{Ox}}}$; (C) E_{SW} = 50 mV, ΔE = 2 mV, $\Phi = \frac{i}{nFSc_{Ox}^*\sqrt{Df}}$.

potential (in both directions), to which potential pulses (of defined amplitude) are superimposed. Currents are measured before (I_1) and at the end (I_2) of each pulse, and the difference ($\Delta I = I_2 - I_1$)

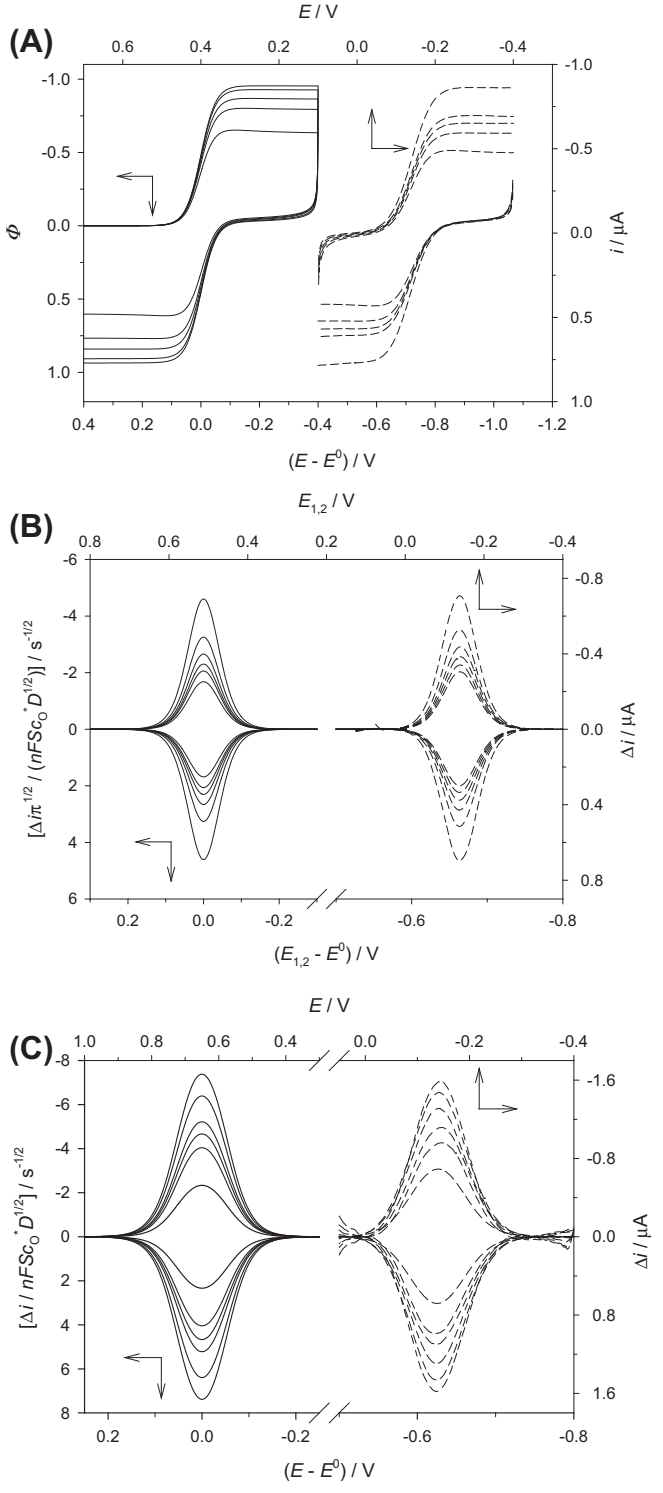

Fig. 3. Dependence of the (-) theoretical and (- -) experimental: (A) cyclic multipulse voltammograms on the interval time, (B) cyclic differential multipulse voltammograms on the pulse duration and C) cyclic square-wave voltammograms on the SW frequency, for reversible electrode reaction (1). (A) E_{st} = 0.4 V vs. E^0, E_S = −0.4 V vs. E^0, ΔE = 2 mV, t_p = 50 ms, n = 1, t_d/s (for negative scan direction, in the ascending order) = 0.10, 0.15, 0.20, 0.30 and 0.40. (B) E_{st} = 0.6 V vs. E^0, E_S = −0.6 V vs. E^0, t_d = 0.15 s, ΔE = 2 mV, E_{DMPV} = 50 mV and t_p/ms (for negative scan direction, in the descending order) = 10, 20, 30, 40, 50 and 75 (C) E_{st} = 0.3 V vs. E^0, E_S = −0.3 V vs. E^0, E_{SW} = 50 mV, ΔE = 2 mV and f (for negative scan direction, in the ascending order) = 10, 30, 40, 50, 75 and 100 s^{-1}. Experiment: $c(UO_2^{2+})$ = 0.3 mmol/L, $c(NaClO_4)$ = 3 mol/L, pH = 2.7, E_{st} = 0.1 V, E_S = −0.4 V.

is plotted against the staircase potential, as in the classical DPV [16,24,25]. Opposite to Drake at al. [11], we used the same

(absolute) values but different signs of the pulse amplitude and step potential in negative and positive scan directions. The net cyclic differential multipulse voltammogram, obtained in such a way, consists of two peaks at different sides of the potential axis (Fig. 2B), unlike the results given in ref. [11] where two peaks (from the forward and reverse scans) were overlapped.

In CSWV potential-time excitation waveform includes stepwise change of the electrode potential, initially in the negative and then to positive direction (as in CMPV and CDMPV), to which square-wave sequence of potential pulses (of defined amplitude) are superimposed. The current is measured at the end of each pulse (in both scan directions) and the difference between currents measured on two successive pulses is recorded as a net response ($\Delta\Phi = \Phi_f - \Phi_b$) and plotted as a function of the staircase potential. The net cyclic square-wave voltammogram of the reversible reaction (1) consists of two symmetric peaks at $E_p = E^0$ (Fig. 2C), which reflect the reduction of the reactant Ox and reoxidation of the product Red.

As can be seen in Fig. 2, the ratio between cathodic and anodic diffusion/limiting currents (in CMPV) as well as the ratio between the net peak currents (in CDMPV or CSWV) is (approximately) equal to unity, regardless of the values of specific timing parameters (i.e. t_p, t_d or f) (Fig. 3) although in CMPV some additional conditions, concerning the ratio between t_p and t_d should be fulfilled [26]. The mentioned type of results and the linear dependence of the net peak (diffusion) current on $t_p^{-1/2}$ (i.e. $f^{1/2}$), are characteristics of a simple reversible electrode reaction with both components of the redox pair dissolved in the electrolyte solution. Moreover, the difference between the cathodic and anodic half-wave potentials (in CMPV) and the difference between the net peak potentials (in CSWV) are equal to 0 V, whereas in CDMPV its value is equal to the applied pulse amplitude. Another possibility, for comparing CDMPV with CSWV, is to use "medium" potential (i.e. $E_{1,2} = (E_1 + E_2)/2$ where E_1 denotes prepulse (staircase) electrode potential whereas E_2 is pulse potential) as the x-axis of the response. In this way, both cathodic and anodic peaks of the net CDMP voltammogram become centered at the formal potential for reversible electrode reaction, i.e. $E_{p,c} = E_{p,a} = E^{0'}$ (same as in CSWV, see the right voltammogram in Fig. 2B and C). Therefore, further in text all other CDMPV signals are shown in this way. More about benefits of such presentation of experimental and theoretical voltammograms can be found in Ref. [27].

Theoretical results were examined and verified for the reversible electrochemical reaction of $UO_2^{2+} + e^- \leftrightarrow UO_2^+$ in acidified (pH ~ 3) 3 mol/L $NaClO_4$ solution. A very good agreement between the experiment and theory was obtained. More exactly, $\Delta i_{p,a}/\Delta i_{p,c}$ (as well as $i_{d,a}/i_{d,c}$) = 1 and $\Delta E_{1/2(p,SWV)} = 0$ mV whereas $\Delta E_{p,DMPV} = 50 \pm 2$ mV in measurements with $E_{DMPV} = 50$ mV (or $\Delta E_{p,DMPV} = 0$ mV if the "medium" potential is used as the x-axis), for all values of the timing parameters.

4.2. Kinetically controlled electrode reactions

The influence of the charge transfer kinetics on theoretical cyclic multipulse voltammograms was studied.

4.2.1. Cyclic multi pulse voltammetry (CMPV)

In CMPV the cathodic and anodic limiting currents do not depend on dimensionless kinetic parameter, $\kappa = k_s(t_p/D)^{1/2}$, i.e. they reach the same (absolute) values and the ratio $|i_{d,a}/i_{d,c}| \approx 1$, for all values of κ. These currents could be useful for determination of the bulk concentrations or diffusion coefficients of both redox components as well as the electrode radius [6,26]. Additionally, under the influence of electrode kinetics the forward/cathodic branch of the voltammogram consists of only one wave whose position on the potential axes depends on the value of kinetic parameter. On the other hand, the reverse/anodic branch of the same voltammogram consists of two waves (see inset in Fig. 4): a cathodic wave corresponding to reduction of the reactant Ox and an anodic one related to (re)oxidation of the product Red electrogenerated during the time τ, at $E_S \ll E^0$. Both half-wave potentials ($E_{1/2,rc}$ and $E_{1/2,ra}$) also depend on the value of κ. Diminishing the values of κ, cathodic/forward and anodic/reverse waves of the current response become more separated.

The theoretical influence of κ was investigated for the following set of standard parameters: $t_d = 0.4$ s, $t_p = 50$ ms, $E_{st} = 0.3$ V vs. E^0,

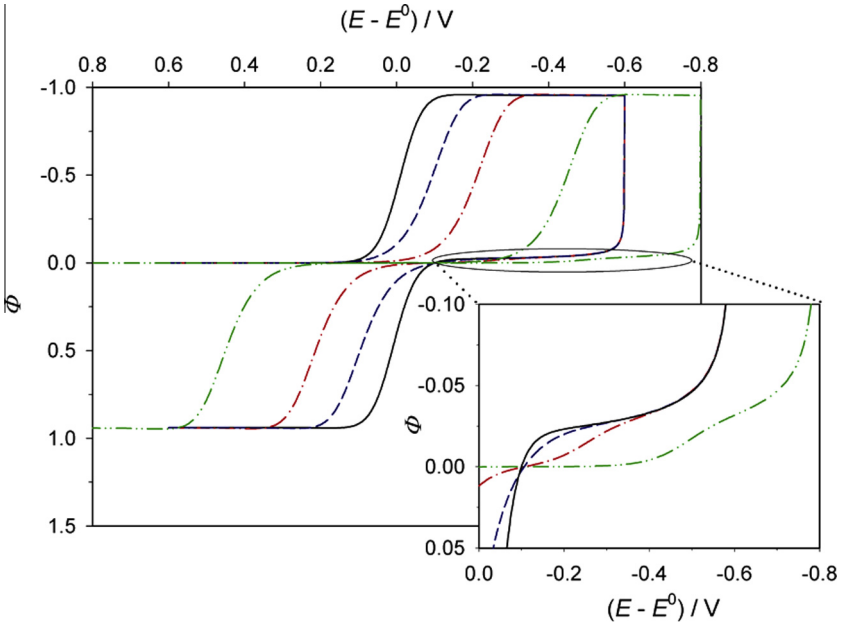

Fig. 4. Influence of the dimensionless kinetic parameter, κ, on theoretical cyclic multipulse voltammograms. $n = 1$, $\alpha = 0.5$, $t_d = 0.4$ s, $t_p = 50$ ms, $\Delta E = 2$ mV, κ (for negative scan direction) = 0.7, 0.07, 0.007 and 0.0007.

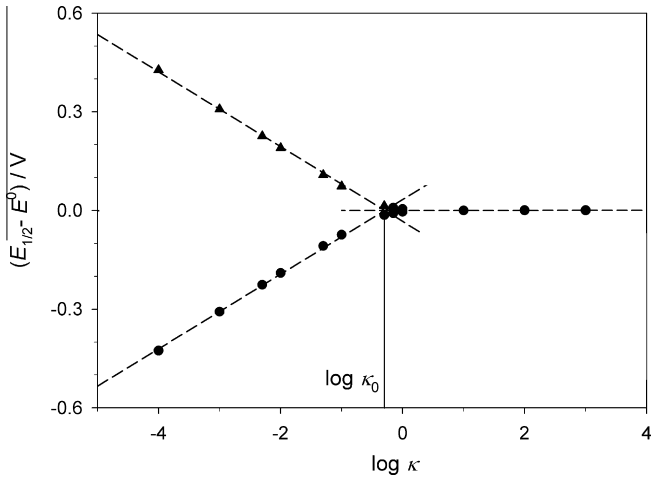

Fig. 5. Theoretical dependence of the reduction (●) and oxidation (▲) half-wave potentials of the CMP voltammograms on the logarithm of kinetic parameter. ΔE = 2 mV, t_d = 0.4 s, t_p = 50 ms, n = 1 and α = 0.5.

E_S = −0.6 vs. E^0. The simulations were performed for n = 1, and for various values of transfer coefficient: 0.1 < α < 0.9.

Fig. 5 shows the relationships between half-wave potentials of both waves (i.e. cathodic/forward and anodic/reverse) in CMPV and the logarithm of kinetic parameter. If log κ < −0.3 these relationships are linear and the slopes of straight lines are:

$$\frac{\partial E_{1/2,c}}{\partial \log \kappa} = \frac{m}{\alpha n} = 0.113 \tag{2}$$

$$\frac{\partial E_{1/2,a}}{\partial \log \kappa} = -\frac{m}{(1-\alpha)n} = -0.114 \tag{3}$$

where m is a constant. Its value was determined, by calculating the relationships between half-wave potentials and the dimensionless kinetic parameters, for three values of the transfer coefficient: α = 0.25, 0.5 and 0.75. The average value of the constant is: m = (0.0562 ± 0.0023) V.

In CMPV the electrode reaction (1) appears reversible (i.e. $E_{1/2,c} = E_{1/2,a} = E^0$) if log$\kappa$ > −0.3. The intercept of the straight lines: $E_{1/2,c}$ = 0.033 + 0.113 log(κ) and $E_{1/2,a}$ = −0.033 − 0.114 log(κ) with line $E_{1/2} = E^0$ is marked as log(κ_0) and presents the critical value of the kinetic parameter, i.e. the lowest value of κ for which $E_{1/2(p)} = E^0$.

The advantage of CMPV over the NPV and RPV is, among others, the possibility for the simultaneous determination of both cathodic (α) and anodic ($\beta = 1 - \alpha$) transfer coefficients from two different data sets.

The influence of the transfer coefficient α on dimensionless CMP voltammograms (in case of kinetically controlled electrode reaction (1)) as well as the relationships between the cathodic and anodic half-wave potentials and the reciprocities of α and $(1 - \alpha)$ are shown in Fig. 6. As can be seen, the transfer coefficient affects the shape and the slope of CMPV signal, so that both cathodic/forward and anodic/reverse waves shift towards more negative potentials as the value of α diminishes. This means that for α < 0.5 oxidation (and for α > 0.5 reduction) is the energy more favorable process. Thus, the response in CMPV reflects symmetry of the electron transfer i.e. gives a qualitative information about the transfer coefficient and apparent rate of the electrode reaction. Furthermore, as can be seen from the inset in Fig. 6 both relationships (i.e. the dependences of the reduction and oxidation half-wave potentials on $1/\alpha$ and $1/(1 - \alpha)$) are linear and pass through the origin: $E_{1/2,c} - E^0 = -0.036/\alpha n$ V and $E_{1/2,a} - E^0 = 0.036/(1 - \alpha)n$ V. The fact that these straight lines have no intercept means that the intercepts of all linear relationships shown in Fig. 5 are functions of either $(\alpha n)^{-1}$, or $((1 - \alpha)n)^{-1}$, i.e. for cathodic/forward branch of the CMP voltammogram:

$$E_{\frac{1}{2},c} - E^0 = \frac{m}{\alpha n}\log\kappa + \frac{\text{const}}{\alpha n} \tag{4}$$

Introducing the value of m into Eq. (4) one obtains:

$$-0.036 = 0.0562 \cdot \log\kappa + \text{const} \tag{5}$$

i.e. considering that logκ = −1 (Fig. 6), the value of constant is 0.0202 V. These calculations were repeated for logκ = −1.5 and logκ = −2 and the average values of intercepts of straight lines shown in Fig. 5 were determined:

$$E_{\frac{1}{2},c} - E^0 = \frac{m}{\alpha n}\log\kappa + \frac{0.0193 \pm 0.0009}{\alpha n} \tag{6}$$

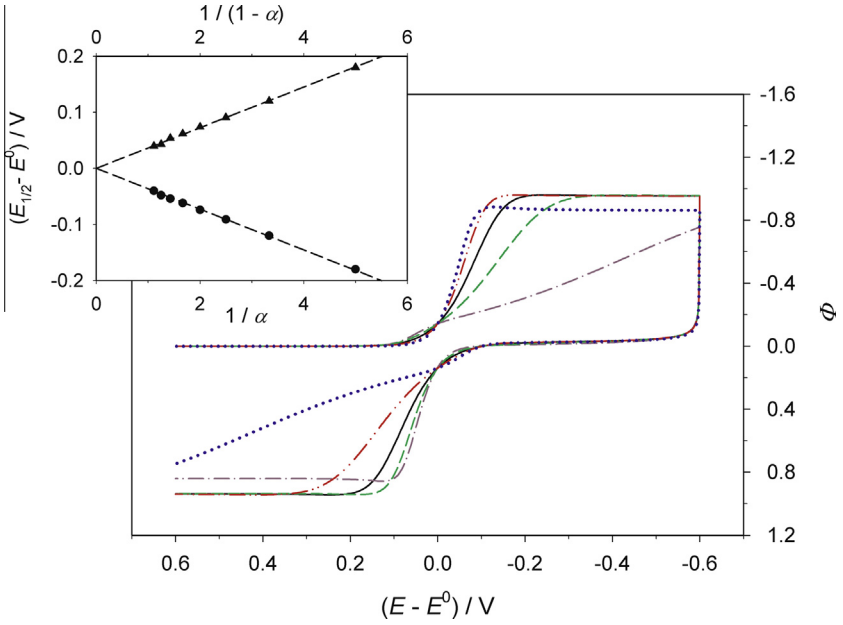

Fig. 6. Influence of the electron transfer coefficient on the CMP voltammograms. ΔE = 2 mV, t_d = 0.4 s, t_p = 50 ms, n = 1, κ = 0.1, α = 0.9 (· · ·), 0.7 (—· ·—), 0.5 (—), 0.3 (— —) and 0.1 (—·· ··—). Inset: dependence of the reduction (●) and oxidation (▲) half-wave potentials on the $1/\alpha$ and $1/(1 - \alpha)$, respectively.

$$E_{\frac{1}{2},a} - E^0 = -\frac{m}{(1-\alpha)n}\log\kappa - \frac{0.019 \pm 0.0006}{(1-\alpha)n} \quad (7)$$

Considering that the critical kinetic parameter, κ_0, gives the lowest value of κ for which $E_{1/2,c} = E_{1/2,a} = E^0$, from Eqs. (6) and (7) its value is:

(a) For cathodic/forward wave of CMP voltammogram:

$$\log\kappa_0 = -\frac{0.0193 \pm 0.0009}{0.0562} = -0.343 \pm 0.016 \quad (8)$$

(b) For anodic/backward wave of CMP voltammogram:

$$\log\kappa_0 = -\frac{0.019 \pm 0.0006}{0.0562} = -0.338 \pm 0.011 \quad (9)$$

Experimentally, variation of the kinetic parameter κ is achieved by changing the pulse duration, t_p, i.e. the half-wave potentials are plotted in dependence of the logarithm of pulse duration. The critical pulse duration $t_{p,0}$ and the critical kinetic parameter are connected by the following equation:

$$\log\kappa_0 = \log k_s - \frac{1}{2}\log D + \frac{1}{2}\log t_{p,0} \quad (10)$$

So, if the formal potential is known, the standard rate constants of the reduction/forward and oxidation/reverse electrode reactions could be determined by the variation of t_p:

$$\log k_{s\frac{Ox}{Red}} = \frac{1}{2}\log D - \frac{1}{2}\log t_{p,0} - 0.343 \pm 0.016 \quad (11)$$

$$\log k_{s\frac{Red}{Ox}} = \frac{1}{2}\log D - \frac{1}{2}\log t_{p,0} - 0.338 \pm 0.011 \quad (12)$$

where the value of D can be determine from the limiting (cathodic and anodic) currents of the CMP voltammogram, by Cottrell equation [28].

4.2.2. Cyclic differential multi pulse voltammetry (CDMPV)

The influence of charge transfer kinetics on cyclic differential multipulse voltammograms of electrode reaction (1) is shown in Fig. 7. The theoretical influence of dimensionless kinetic parameter ($\kappa = k_s\sqrt{\frac{t_p}{D}}$) was investigated for the following set of standard parameters: $t_d = 0.15$ s, $t_p = 25$ ms, $nE_{DMPV} = 50$ mV, $\Delta E = 5$ mV, $E_{st} = 0.6$ V vs. E^0, $E_S = -0.6$ vs. E^0. The simulations were performed for $n = 1$, and for various values of transfer coefficient: $0.1 < \alpha < 0.9$.

As expected, both cathodic and anodic peaks of the net CDMP voltammogram become more separated, and their currents more reduced, as the value of κ decreases. In other words, these effects and the ratio $|\Delta i_{p,a}/\Delta i_{p,c}| < 1$ (for all values of t_p) indicate decreased reversibility of the electrode process. On the other hand, dependence of the normalized net peak currents ($\Delta\Phi_p t_p^{-1/2}$) of CDMPV signal for quasireversible (as well as for reversible) electrode reaction (1) is a linear function of $t_p^{-1/2}$, while the slope of corresponding straight line depends on electron transfer kinetics (i.e. a decreased slope of the "reverse peak currents" dependence for quasireversible reaction, is observed).

Furthermore, it can be seen that in the case of "slow" electrode process (i.e. for $\kappa \leqslant 10^{-2}$), reverse branch of the net response, splits in two peaks: cathodic and anodic one (same as in the CSWV, see Fig. 10). Cathodic/reverse peak corresponds to reduction of the reactant Ox for $E_{1,2} - E^0 < -160$ mV. Its positive value of the net current (which could lead to wrong conclusion about the character of redox process) results from the way of current recording/displaying, as a difference between the "pulse" and "prepulse" components (i.e. $\Delta\Phi = \Phi_2 - \Phi_1$, where $\Phi_2 > \Phi_1$, and both components are reductive currents, in this potential range). On the other hand, both current components of the anodic/reverse peak are positive (at the potentials $E > E^0$) which indicates that this peak originates from the oxidation of the product Red. The maximum current of the cathodic/reverse peak is lower than the anodic one, as a result of the concentration gradient of the redox components in diffusion layer, i.e. the concentration of the reactant Ox is diminished during the forward reduction reaction. This holds for the examined parameters, whereas it is expected that the relationship between

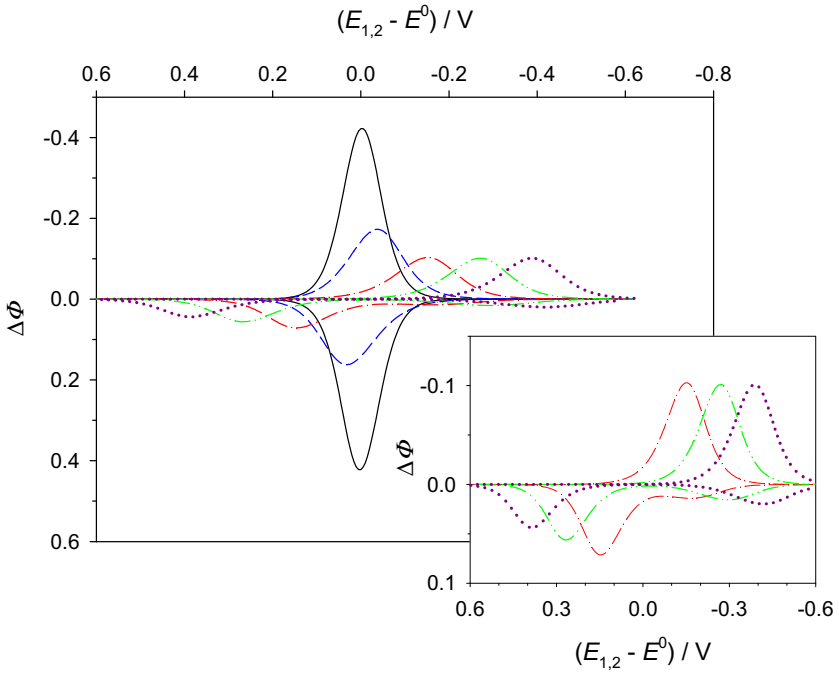

Fig. 7. Influence of the dimensionless kinetic parameter, κ, on theoretical cyclic differential multipulse voltammograms. $n = 1$, $\alpha = 0.5$, $t_d = 0.15$ s, $t_p = 25$ ms, $E_{DMPV} = 50$ mV, $\Delta E = 5$ mV, κ (for negative scan direction) = 1, 0.1, 0.01, 0.001 and 0.0001. Inset: the theoretical CDMP voltammograms for $\kappa = 0.01$, 0.001 and 0.0001.

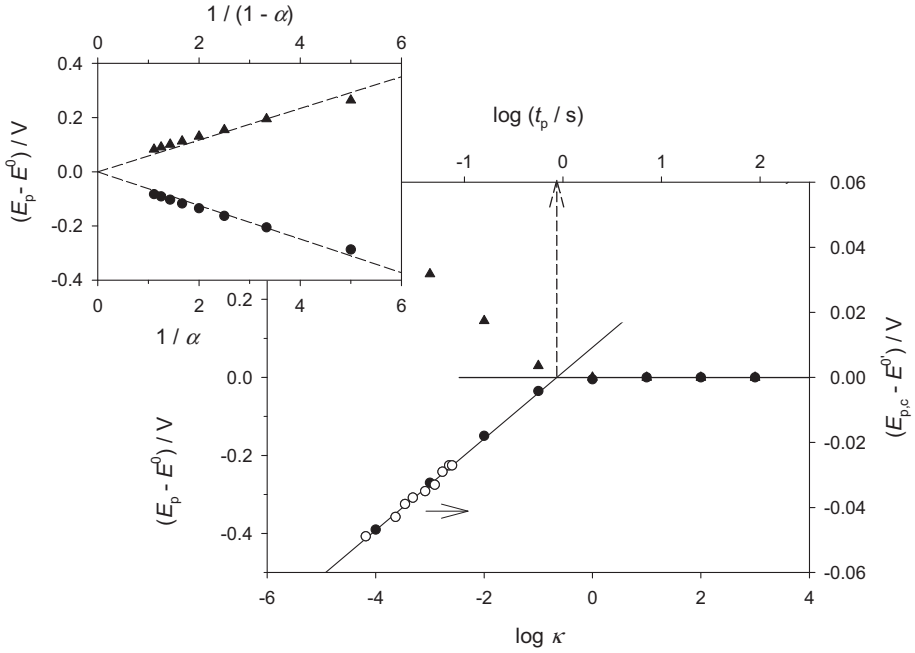

Fig. 8. Theoretical dependence of the reduction (●) and the oxidation (▲) peak potentials of the CDMP voltammogram on the logarithm of kinetic parameter. E_{DMPV} = 50 mV, ΔE = 5 mV, t_d = 0.15 s, t_p = 25 ms, n = 1 and α = 0.5. Experimental dependence of the reduction (○) peak potential on logarithm of pulse duration for Eu^{3+}/Eu^{2+} system. $c(Eu^{3+})$ = 0.2 mmol/L, $c(NaClO_4)$ = 0.1 mol/L, $c(HClO_4)$ = 0.01 mol/L, ΔE = 2 mV, E_{DMPV} = 50 mV, t_d = 0.15 s, t_p = 10–75 ms, S = 0.26 mm^2, $E^{0'}(Eu^{3+}/Eu^{2+})$ = −0.598 V; $\log(t_{p,0}/s)$ = −0.066 (Inset: theoretical dependence of the reduction (●) and oxidation (▲) net peak potentials on the $1/\alpha$ and $1/(1-\alpha)$, respectively. ΔE = 2 mV, κ = 0.01).

these peaks additionally depends on the step potential, ΔE (in the same way as in the reverse SWV [29]).

The difference between the cathodic peak potentials obtained by scanning in both directions, of the net CDMPV response, is rather small, i.e. $\Delta E_{p,c}$ = 20 ± 10 mV for examined kinetic parameters. Therefore in this study each theoretical dependence is expressed as the difference or the ratio between the anodic/reverse and cathodic/forward peaks. The current ratio $\Delta\Phi_{p,a}/\Delta\Phi_{p,c}$ is not a linear function of the logarithm of kinetic parameter (for $\log\kappa < 0$) (i.e. current ratio nonlinearly decreases, as the κ values diminishes).

Fig. 8 shows the relationships between the net peak potentials of CDMP voltammogram and the logarithm of kinetic parameter. (The relationship between potentials of the cathodic and the anodic peak of CDMPV net response and α^{-1} and $(1-\alpha)^{-1}$, respectively, are shown in the inset). If $\log\kappa \leqslant -1$ these relationships are linear and the slopes of straight lines are:

$$\frac{\partial E_{p,c}}{\partial \log\kappa} = \frac{2.3RT}{\alpha nF} = 0.119 \tag{13}$$

$$\frac{\partial E_{p,a}}{\partial \log\kappa} = -\frac{2.3RT}{(1-\alpha)nF} = -0.118 \tag{14}$$

In CDMPV the electrode reaction (1) appears reversible (i.e. $|\Delta i_{p,a}/\Delta i_{p,c}| = 1$, and $\Delta E_p = E_{DMPV}$) if $\log(\kappa) \geqslant 0$. Within the range $-2 < \log\kappa < 0$ the reaction (1) is quasireversible.

Furthermore, the relationships between potentials of cathodic and anodic peaks of net response and reciprocities of α and $(1-\alpha)$, are linear and pass through the origin: $E_{p,c} - E^0 = -0.054/\alpha n$ V and $E_{p,a} - E^0 = 0.050/(1-\alpha)n$ V, which means that the intercepts of all linear relationships shown in this figure are functions of either $(\alpha n)^{-1}$, or $((1-\alpha)n)^{-1}$. For instance:

$$E_{p,c} - E^0 = \frac{2.3RT}{\alpha nF}\log\kappa + \frac{\text{const.}}{\alpha n} \tag{15}$$

Comparing Eq. (15) and inset in Fig. 8 one obtains:

$$-0.054 = 0.059\log\kappa + \text{const.} \tag{16}$$

Considering that $\log\kappa = -2$ (inset in Fig. 8), the value of constant is 0.064 V. These calculations were repeated for $\log\kappa = -2.5$ and $\log\kappa = -3$ and the average values of intercepts of straight lines shown in Fig. 8 were determined:

$$E_{p,c} - E^0 = \frac{2.3RT}{\alpha nF}\log\kappa + \frac{0.066 \pm 0.002}{\alpha n} \tag{17}$$

$$E_{p,a} - E^0 = -\frac{2.3RT}{(1-\alpha)nF}\log\kappa - \frac{0.070 \pm 0.003}{(1-\alpha)n} \tag{18}$$

The critical kinetic parameters κ_0 correspond to $E_{p,c} = E^0$, $E_{p,a} = E^0$, etc.

(a) For $E_{p,c}$:

$$\log\kappa_0 = -\frac{0.066 \pm 0.002}{0.059} = -1.12 \pm 0.03 \tag{19}$$

(b) For $E_{p,a}$:

$$\log\kappa_0 = -\frac{0.070 \pm 0.003}{0.059} = -1.19 \pm 0.05 \tag{20}$$

The critical pulse duration $t_{p,0}$ and the critical kinetic parameter κ_0 are connected by Eq. (10), i.e. if the formal potential is known, the standard rate constant can be determined by variation of the pulse duration (in the same way as in CMPV). Thus, if the cathodic/forward peak potential $E_{p,c}$ is used in these calculations, the critical kinetic parameter is defined by Eq. (19):

$$\log k_{s_{\frac{Ox}{Red}}} = \frac{1}{2}\log D - \frac{1}{2}\log t_{p,0} - 1.12 \pm 0.03 \tag{21}$$

i.e. for the anodic/reverse peak:

$$\log k_{s_{\frac{Red}{Ox}}} = \frac{1}{2}\log D - \frac{1}{2}\log t_{p,0} - 1.19 \pm 0.05 \tag{22}$$

For that reason, the influence of parameter t_p on CDMP voltammograms, for quasireversible electrode reaction of europium (+3) in acidified 0.1 mol/L $NaClO_4$ [30], was examined. It can be seen

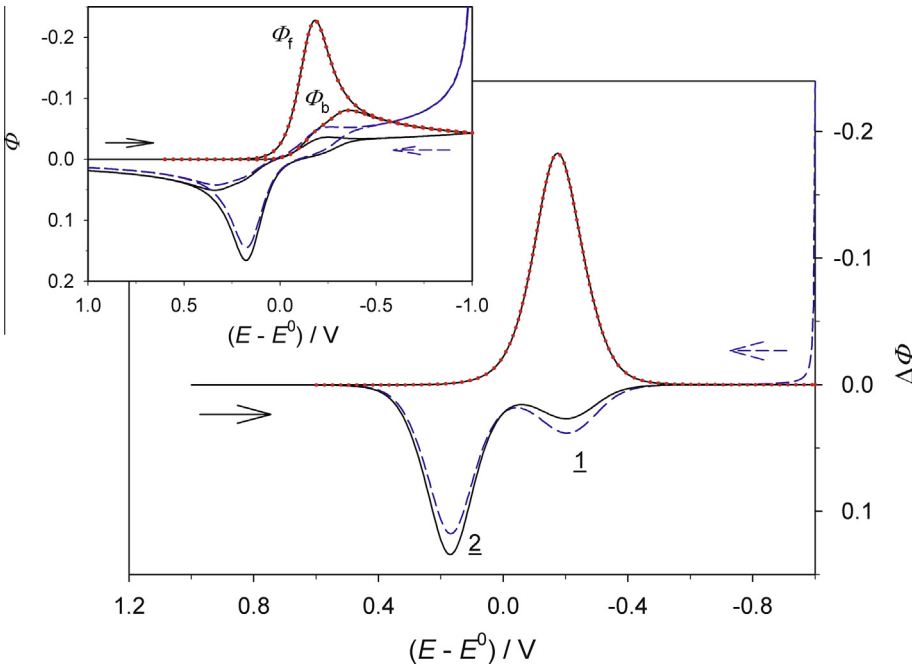

Fig. 9. Theoretical square-wave voltammograms of electrode reaction (1) calculated for the "negative" (· · ·), "positive" (- - -) and "cyclic" (-) potential scan directions, along with their, Inset: forward (Φ_f) and backward (Φ_b) current components. E_{SW} = 50 mV, n = 1, κ = 0.01, α = 0.5, ΔE = 5 mV, $\Phi = \frac{i}{nFSc_0^*\sqrt{Df}}$.

that experimentally obtained dependence of the cathodic peak potentials on the logarithm of pulse duration is in good agreement with theoretical for kinetically controlled electrode process. Introducing the values of $D_{Eu3+} = 6.7 \times 10^{-6}$ cm^2 s^{-1} (calculated from the limiting/cathodic current of CMPV by Cottrell eq.) and log($t_{p,0}$/s) = −0.066 (Fig. 8) in Eq. (21) the standard rate constant for redox system Eu^{3+}/Eu^{2+} is obtained: $k_s = (2.11 \pm 0.14) \times 10^{-4}$ cm s^{-1} (where $E^{0\prime}_{Eu3+/Eu2+} = -0.598$ V has been taken as a mean value of the literature data [31,32], recalculated vs. Ag/AgCl (3.5 mol/L KCl) reference electrode). This value of the k_s is in a relatively good agreement with the published value ($k_s = 1.7 \times 10^{-4}$ cm s^{-1} [31]).

Furthermore, the cathodic (α) and anodic (β) transfer coefficients can be calculated from the slopes of linear relationships between cathodic/forward and anodic/reverse peak potentials of the net CDMPV response and the logarithm of pulse duration (see Eqs. (13) and (14)).

4.2.3. Cyclic square-wave voltammetry (CSWV)

According to our previous investigations [9,33] the combination of negative/direct and positive/reverse scan directions in square-wave voltammetry enables complete characterization of apparently irreversible electrode reaction. In this study we show that the net peak currents of reverse scan SWV and the "reverse" branch of the CSWV are more or less different. Fig. 9 shows the difference between theoretical SW voltammograms of an apparently irreversible electrode reaction (1) calculated for the negative ("classic"), positive ("reverse") and cyclic potential scan directions. The observed differences in the net peak currents are caused by concentration gradient of the reactant Ox in diffusion layer. More exact, in CSWV at the switching potential ($E_S \ll E^0$) concentration of the reactant Ox near the electrode surface is rather small as a consequence of forward reduction reaction, i.e. during the cathodic and anodic pulse potentials (in the reverse scan) a small reductive current is flowing through the cell (Φ_f and $\Phi_b \leqslant 0$). The second net peak originates from the oxidation of the product Red (i.e. Φ_f and $\Phi_b > 0$). On the other hand, in reverse scan SW voltammetry at the starting potential ($E_{st} \ll E^0$) the instant reduction of the reactant Ox takes place, which is manifested by high jump of the reductive current (i.e. Φ_f and $\Phi_b < 0$). For this reason the reduction peak (1) is higher and the reoxidation peak (2) is smaller in reverse scan SWV, than the same peaks in CSWV (for a given set of the parameters).

Two peaks of the net response (in reverse and cyclic SWV) are caused by the pronounced separation between the forward and backward components of the net current.

The influence of electron transfer kinetics on cyclic square-wave voltammograms of electrode reaction (1) is shown in Fig. 10. The theoretical influence of the dimensionless kinetic parameter ($\kappa = k_s(Df)^{-1/2}$) was investigated for the following set of standard parameters: E_{SW} = 50 mV, ΔE = 5 mV, E_{st} = 1 V vs. E^0. The simulations were performed for three values of the number of exchanged electrons, n = 1, 2 and 3, and for various values of transfer coefficient: $0.1 < \alpha < 0.9$.

In agreement with our previous findings [33], the same relationships between characteristic peak potentials ($E_{p,c}$, $E_{p,1}$ and $E_{p,2}$) of the net CSW voltammogram and the logarithm of kinetic parameter could be noted (i.e. Eqs. (2)–(15) in [33] are applicable as well). Accordingly, the cathodic transfer coefficients (α = 0.76), for quasireversible electrode reaction of europium (+3) in acidified 0.1 mol/L $NaClO_4$, is obtained from the slopes of linear relationships between cathodic/backward peak potentials ($E_{p,1}$) of the net CSWV response and the logarithm of SW frequency (analog to Eq. (13)). This value of α is in perfect agreement with our previous results [9] and good agreement with a literature value [34]. Furthermore, the maximum currents of all peaks of CSWV net response increase nonlinearly if the SW amplitude (E_{SW}) is increased.

5. Conclusions

The signals that arise from the application of cyclic multi pulse voltammetry, cyclic differential multi pulse voltammetry and cyclic square-wave voltammetry were simulated.

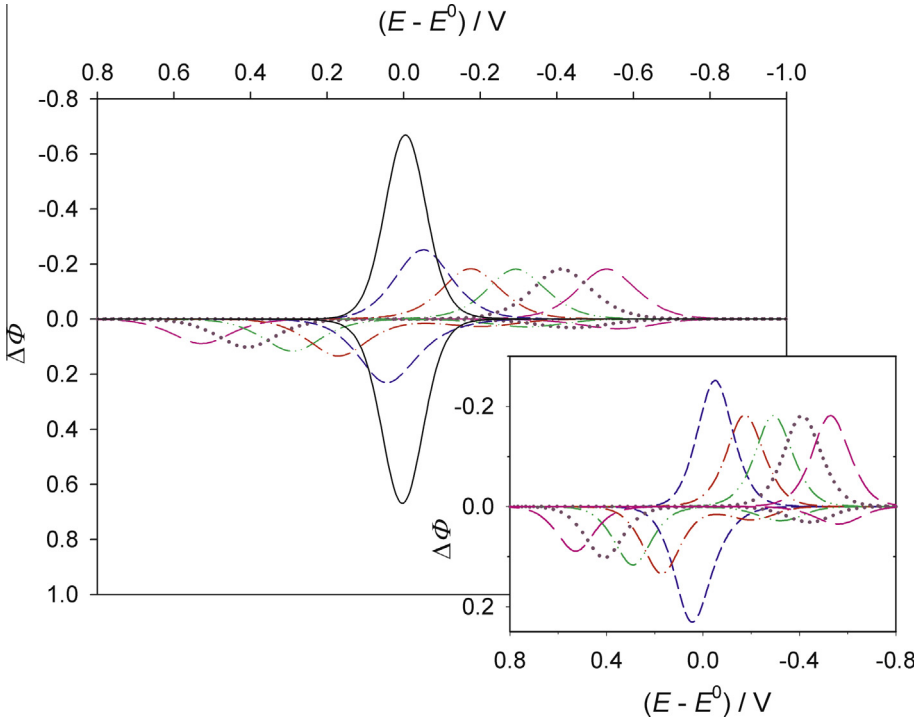

Fig. 10. Influence of the dimensionless kinetic parameter, κ, on theoretical cyclic square-wave voltammograms. $n = 1$, $\alpha = 0.5$, $E_{SW} = 50$ mV, $\Delta E = 5$ mV, κ (for negative scan direction) = 1, 0.1, 0.01, 0.001, 0.0001 and 0.00001.

The criteria for recognition of reversible and kinetically controlled electrode reactions are given:

	CMPV	CDMPV	CSWV
Reversible	$i_{d,a}/i_{d,c} = 1$	$\Delta i_{p,a}/\Delta i_{p,c} = 1$	$\Delta i_{p,a}/\Delta i_{p,c} = 1$
	$\Delta E_{1/2} = 0$ V	$\Delta E_p = 0$ V	$\Delta E_p = 0$ V
None-reversible	$i_{d,a}/i_{d,c} < 1$	$\Delta i_{p,a}/\Delta i_{p,c} < 1$	$\Delta i_{p,a}/\Delta i_{p,c} < 1$
	$\lvert\Delta E_{1/2}\rvert > 0$ V	$\lvert\Delta E_p\rvert > 0$ V	$\lvert\Delta E_p\rvert > 0$ V

From the theoretical and experimental analysis, it follows that the cyclic multipulse voltammetric techniques enable fast and complete characterization of the electrode processes. The cyclic multipulse voltammograms of a simple kinetically controlled electrode reaction $O_{(aq)} + ne^- \rightleftarrows R_{(aq)}$ consist of one: reduction/forward and two: reduction and (re)oxidation reverse peaks/waves. The standard rate constant, as well as the electron transfer coefficients (α and β), can be determined by the variation of pulse time in CMPV and CDMPV, i.e. by the variation of frequency in CSWV. Therefore, the symmetry and apparent rate of the electron transfer reaction can be estimated by visual inspection of proper cyclic multipulse voltammogram. These are, among others, the advantages of cyclic multipulse techniques with regard to cyclic staircase voltammetry.

Furthermore, the advantage of these techniques (using the SMDE) is a fact that the whole experiment (electro-reduction and -oxidation) is taken at the same mercury drop, which is especially useful if the product of electrode reaction is unstable.

All results in this paper are based on the classical Bultel–Volmer approach, although in recent years, for analyzing the electrode kinetics, the other theoretical approach known as Marcus–Hush–Chidsey model/formalism became a popular [35–37]. However, in accordance with the statement of experts in the field [37]: "the MHC model does not always give a satisfactory fit to experimental data in contrast to BV parameterization", this approach should not be superior in examined processes.

Acknowledgements

The authors would like to thank to Dr. Sc. Milivoj Lovrić for helpful discussion and advices.

Financial support of the Ministry of Science, Education and Sports of the Republic of Croatia within the projects *Electroanalytical Investigations of Microcrystals and Traces of Dissolved Compounds* is gratefully acknowledged.

References

[1] G.C. Barker, A.W. Gardner, Fresenius Z. Anal. Chem. 173 (1960) 79–83, and references therein.
[2] J.E. Anderson, A.M. Bond, Anal. Chem. 55 (1983) 1934–1939, and references therein.
[3] M.D. Ryan, J. Electroanal. Chem. 79 (1977) 105–119.
[4] L.-H.L. Miaw, P.A. Boudreau, M.A. Pichler, S.P. Perone, Anal. Chem. 50 (1978) 1988–1996.
[5] J. Osteryoung, E. Kirowa-Eisner, Anal. Chem. 52 (1980) 62–66.
[6] A. Molina, F. Martinez-Ortiz, E. Laborda, R.G. Compton, J. Electroanal. Chem. 648 (2010) 67–77.
[7] Z. Stojek, J. Electroanal. Chem. 256 (1988) 283–289.
[8] N. Fatouros, D. Krulic, J. Electroanal. Chem. 520 (2002) 1–5.
[9] M. Zelić, Croat. Chem. Acta 79 (2006) 49–55.
[10] N. Fatouros, D. Krulic, N. Larabi, J. Electroanal. Chem. 568 (2004) 55–64.
[11] K.F. Drake, R.P. van Duyne, A.M. Bond, J. Electroanal. Chem. 89 (1978) 231–246.
[12] C. Xinsheng, P. Guogang, Anal. Lett. 20 (1987) 1511–1519.
[13] L. Camacho, J.J. Ruiz, C. Serna, A. Molina, J. Gonzalez, J. Electroanal. Chem. 422 (1997) 55–60.
[14] A. Molina, M.M. Moreno, C. Serna, M. Lopez-Tenes, J. Gonzales, N. Abenza, J. Phys. Chem. C 111 (2007) 12446–12453.
[15] J.C. Helfrick Jr., L.A. Bottomley, Anal. Chem. 81 (2009) 9041–9047.
[16] A. Molina, E. Laborda, F. Martinez-Ortiz, D.F. Bradley, D.J. Schiffrin, R.G. Compton, J. Electroanal. Chem. 659 (2011) 12–24.
[17] Gmelin's Handbuch der Anorganischen Chemie, 8th ed., No. 55, Verlag Chemie, Weinheim, 1936, p. 136.
[18] NOVA 1.7. Dedicated to research, User manual, Metrohm Autolab, 2005–2010.
[19] B. Speiser, in: A.J. Bard, I. Rubinstein (Eds.), Electroanalytical Chemistry, vol. 19, Dekker, New York, 1996, pp. 2–99.
[20] A.J. Bard, L.R. Faulkner, Electrochemical methods fundamentals applications, 2nd ed., Wiley, New York, 2001.
[21] S. Sujaritvanichpong, K. Aoki, K. Tokuda, H. Matsuda, J. Electroanal. Chem. 199 (1986) 271–283.
[22] A.M. Garrigosa, J.M. Diaz-Cruz, C. Arino, M. Esteban, Electrochim. Acta 53 (2008) 5579–5586.

[23] Z. Stojek, in: F. Scholz (Ed.), Electroanalytical Methods. Guide to Experiments and Applications, 2nd ed., Springer, Heidelberg, 2009, pp. 107–119.
[24] R.G. Compton, C.E. Banks, Understanding Voltammetry, World Scientific Publishing Co., New Jersey, 2007.
[25] K. Aoki, K. Tokuda, H. Matsuda, J. Electroanal. Chem. 175 (1984) 1–13.
[26] E. Laborda, E.I. Rogers, F. Martinez-Ortiz, C. Serna, J.G. Limon-Petersen, N.V. Rees, A. Molina, R.G. Compton, J. Electroanal. Chem. 634 (2009) 1–10.
[27] A. Molina, E. Laborda, E.I. Rogers, F. Martinez-Ortiz, C. Serna, J.G. Limon-Petersen, N.V. Rees, R.G. Compton, J. Electroanal. Chem. 634 (2009) 73–81.
[28] Z. Galus, Fundamentals of electrochemical analysis, 2nd ed., Ellis Horwood and Polish Scientific Publishers, New York, 1994.
[29] M. Zelić, M. Lovrić, J. Electroanal. Chem. 637 (2009) 28–32.
[30] M. Zelić, Croat. Chem. Acta 76 (2003) 241–248.
[31] E. Laborda, E.I. Rogers, F. Martinez-Ortiz, A. Molina, R.G. Compton, Electrochim. Acta 55 (2010) 6577–6585.
[32] M.J. Weaver, F.C. Anson, J. Electroanal. Chem. 65 (1975) 711–735.
[33] M. Lovrić, D. Jadreško, Electrochim. Acta 55 (2010) 948–951.
[34] H. Elzanowska, Z. Galus, Z. Borkowska, J. Electroanal. Chem. 157 (1983) 251–268.
[35] M.C. Henstridge, Y. Wang, J.G. Limon-Petersen, E. Laborda, R.G. Compton, Chem. Phys. Lett. 517 (2011) 29–35.
[36] Y. Wang, E. Laborda, M.C. Henstridge, F. Martinez-Ortiz, A. Molina, R.G. Compton, J. Electroanal. Chem. 668 (2012) 7–12.
[37] M.C. Henstridge, E. Laborda, N.V. Rees, R.G. Compton, Electrochim. Acta 84 (2012) 12–20.